A high-fat diet induces a microbiota-dependent increase in stem cell activity in the *Drosophila* intestine

Jakob von Frieling[1], Muhammed Naeem Faisal[1,3], Femke Sporn[1], Roxana Pfefferkorn[1], Stella Solveig Nolte[1,4], Felix Sommer[2], Philip Rosenstiel[2], Thomas Roeder[1,5#]

[1]Zoological Institute, Department of Molecular Physiology, Kiel University, Kiel, Germany
[2]IKMB, UKSH, Kiel University, Kiel, Germany
[3]Current address: University Faisalabad, Pakistan
[4]Current address: University Aarhus, Denmark
[5]German Center for Lung Research, Airway Research Center North, Kiel, Germany

[#]Correspondence: Thomas Roeder, Zoological Institute, Department of Molecular Physiology, Kiel University, Kiel, Germany; Tel.: ++49-431-8804181; Email: troeder@zoologie.uni-kiel.de

Abstract

Over-consumption of high-fat diets (HFDs) is associated with several pathologies. Although the intestine is the organ that comes into direct contact with all diet components, the impact of HFD has mostly been studied in organs that are linked to obesity and obesity related disorders. We used *Drosophila* as a simple model to disentangle the effects of a HFD on the intestinal structure and physiology from the plethora of other effects caused by this nutritional intervention. Here, we show that a HFD triggers activation of intestinal stem cells in the *Drosophila* midgut. This stem cell activation was transient and preceded by induction of JNK signaling in enterocytes. JNK (basket) within enterocytes was essential for activation of stem cells in response to a HFD. Moreover, this nutritional intervention leads to upregulation of the cytokine *upd3* in enterocytes, a reaction that is known to trigger STAT signaling in intestinal stem cells followed by their activation. We also showed that the indigenous microbiota was essential for HFD-induced stem cell activation because this response was blunted in germ-free flies lacking a microbiota. Moreover, chronic HFD feeding of flies markedly altered both the microbiota composition and bacterial load. Although HFD-induced stem cell activity was transient, long-lasting changes to the cellular composition, including a substantial increase in the number of enteroendocrine cells, were observed. Taken together, a HFD enhances stem cell activity in the *Drosophila* gut and this effect is completely reliant on the indigenous microbiota and also dependent on JNK signaling within intestinal enterocytes.

Author summary

High-fat diets have been associated with a plethora of morbidities. The major research focus has been on its effects on obesity related disorders, mostly omitting the intestine,

42 although it is the organ that makes the first contact with all diet components. Here, we
43 aimed to understand the direct effects of HFD on the intestine itself. Using *Drosophila* as a
44 model, we showed that HFD induced a transient activation of intestinal stem cells. This
45 response completely depended on JNK signaling in enterocytes. Mechanistically, we found
46 that HFD induces JNK signaling in enterocytes, which triggers production of the cytokine
47 *upd3*. This, in turn activates STAT signaling in intestinal stem cells, leading to their
48 activation. Surprisingly, we found that a HFD triggered induced stem cell activation
49 critically depends on the indigenous microbiota, as in germ free flies this reaction was
50 completely abolished. Moreover, HFD changed both, composition and abundance of the
51 microbiota. As fecal transfer experiments failed to recapitulate the HFD phenotype, we
52 assume that the increased bacterial load is the major cause for the HFD triggered stem cell
53 activation in the intestine.

54

55

56 ## Introduction

57 High caloric intake and especially high-fat diets (HFDs) are major causes of the epidemic
58 increases in obesity-associated diseases [1]. In addition to metabolically relevant organs,
59 the intestines are particularly susceptible to the effects of HFDs because they are in direct
60 contact with constituents of the diet. Consequently, nutritional interventions directly
61 impact intestinal structure and functionality [2]. Diet-dependent plasticity in the size of the
62 intestines has been reported [3]. Specifically, intestinal size decreases in response to dietary
63 restriction [4], but increases upon re-feeding after a period of starvation [5]. Structural
64 changes in response to HFDs are observed at different levels, ranging from subcellular
65 structures in enterocytes [6] to the cellular composition of the intestinal epithelium [7]. The
66 effects of HFDs on the intestinal structure involve alteration of the activity of intestinal stem
67 cells (ISCs). In mammals, HFDs directly enhance the activity of ISCs, leading to increased
68 villi lengths in the small intestines via a mechanism involving ß-catenin signaling [8]. This
69 HFD-induced activation of ISCs appears to be directly caused by the lipid content of food [3,
70 9]. A recent study showed that food with high lipid contents induces very robust PPAR-δ
71 activation in ISCs and thereby increases the number of mitotically active cells in the
72 intestines [9, 10]. Moreover, this response increases the tumorigenicity of intestinal
73 progenitors [2, 9]. This observation correlates with epidemiological studies showing that
74 different types of diets affect the risk of developing intestinal cancers [11, 12]. Specifically,
75 HFDs increase the prevalence of colon cancers [13, 14]. In this context, deregulated stem
76 cell activities appear to be directly associated with alterations in intestinal JAK/STAT
77 signaling [15].

78 Although the major effects of HFDs on the stemness and tumorigenicity of ISCs seem to be
79 directly mediated by exposure of intestinal epithelial cells to fat components [9], secondary

80 effects are also highly relevant to induction of the complex phenotype that results from
81 chronic consumption of a HFD. One important link between HFDs and disease development
82 is the intestinal microbiota [16-18]. High-fat dietary supplementation alters the abundance,
83 composition, and physiological performance of the microbiota [19-21]. In flies, HFDs
84 increase the microbial abundance in the intestines [22]. Associations between an altered or
85 dysbiotic microbiota composition and metabolic diseases have been repeatedly reported
86 [23, 24]. Furthermore, microbiota transfer experiments revealed that altered microbiota
87 compositions play a causative role in the development of metabolic disorders [25, 26]. In
88 *Drosophila*, a link between a dysbiotic microbiota and the activity of ISCs was reported [27].
89 In this context, age-associated increases in the abundance of a particular microbial colonizer
90 and the infection of specific pathogens trigger induction of stem cell activities [28, 29].
91 Despite this large body of informative studies, knowledge of the mechanisms by which
92 HFDs regulate the activity of ISCs is not comprehensive. Here, we used the fruit fly
93 *Drosophila* as a model and showed that a HFD induces a transient increase in stem cell
94 activity via JNK-dependent activation of cytokine expression in enterocytes. This effect is
95 dependent on the microbiota. Thus, we speculate that HFDs elicit physiological effects not
96 only directly via activating stem cells through exposure to different fat components, but
97 also indirectly via altering the microbiota, especially the bacterial abundance in the
98 intestines.
99

100 **Results**

101 We used the fruit fly *Drosophila melanogaster* as a model to study the effects of a HFD on
102 the structural and physiological characteristics of the intestines. Furthermore, we analyzed
103 the contribution of the microbiota to these alterations. HFD feeding triggered a burst of

104 stem cell activity in the midgut (Fig. 1). We used flies that expressed GFP under the control
105 of the escargot (esg) driver, meaning expression was restricted to ISCs and their direct
106 descendants, i.e., enteroblasts. This analysis revealed that in comparison with flies fed a
107 control diet (CD) (Fig. 1A), short durations of HFD feeding induced substantial expansion of
108 these cell types (Fig. 1B). Quantitative analysis of these cells was performed using flies that
109 expressed luciferase in the same spatial pattern (Fig. 1C). Luminescence increased upon
110 very short durations of HFD feeding, but it decreased over time (Fig. 1C). A similar increase
111 in cell number upon HFD feeding was observed when only enteroblasts were analyzed using
112 flies that expressed GFP under the control of the su(H)GBE-Gal4 driver (Fig. 1D–F). After 3
113 days, more enteroblasts were detected in flies fed a HFD (Fig. 1E) than in flies fed a CD (Fig.
114 1D). Similar results were obtained by quantitative analysis of luciferase expression (Fig. 1F).
115 As observed with esg-specific signals (i.e., ISCs plus enteroblasts), luminescence remained
116 elevated after 7 days of HFD feeding. The effects of different diets on ISC activity were
117 directly evaluated by counting the number of phospho-H3 $(pH3)^+$ cells in the gut. The
118 number of $pH3^+$ cells was increased after 3 days of HFD feeding (Fig. 1H) in comparison with
119 flies fed a CD (Fig. 1G), which was further supported by a quantitative analysis of the
120 numbers of $pH3^+$ cells (Fig. 1I). To evaluate the effects of a HFD on the cellular composition
121 of the intestines, we counted the number of enteroendocrine cells, which are direct
122 descendants of enteroblasts, similar to enterocytes (Fig. 1K). A HFD increased the number
123 of enteroendocrine cells in a time-dependent manner (Fig. 1L). This increase started at day
124 5, peaked at day 7, and was sustained for more than 2 weeks in comparison with flies fed a
125 CD.
126 JNK signaling is a major stress-sensitive signaling pathway in the intestines. Therefore, we
127 tested if a HFD affects activation of JNK signaling (Fig. 2). In comparison with flies fed a CD

128 (Fig. 2A), the level of phosphorylated JNK (pJNK), which corresponds to activated JNK, was
129 increased in flies fed a HFD (Fig. 2B). Furthermore, using a JNK reporter line [30] (4xTRE-
130 dsRed), we showed that the level of fluorescence in the anterior midgut was significantly
131 higher in flies fed a HFD than in flies fed a CD (Fig. 2C). The cytokine upd3, which is directly
132 linked to stem cell activation, is a major target of JNK signaling in enterocytes [31]. Thus, we
133 investigated the effects of a HFD on expression of upd3. Using a reporter line (upd3-
134 Gal4::UAS-GFP), we showed that, in comparison with flies fed a CD (Fig. 2D), expression of
135 *upd3* in enterocytes was increased in flies fed a HFD (Fig. 2E). qRT-PCR revealed that the
136 transcript level of *upd3* was significantly increased in flies fed a HFD (Fig. 2F). To determine
137 whether HFD-induced JNK activation is causally linked with upd3 activation, we
138 investigated if inhibition of JNK signaling via ectopic overexpression of a dominant-negative
139 basket allele (bsk^{DN}) in enterocytes affected *upd3* expression. HFD feeding did not increase
140 *upd3* expression in flies expressing bsk^{DN} in enterocytes (Fig. 2F), implying that activation of
141 JNK upon HFD feeding is responsible for the increase in local *upd3* production and
142 consequently stem cell activation. It is well established that upd3 produced by enterocytes
143 induces proliferation of ISCs via activation of JAK/STAT signaling. Therefore, we used a
144 STAT reporter line, in which GFP expression indicates JAK/STAT pathway activation [32]. As
145 expected, GFP was detected in cells with a stem cell-like appearance scattered throughout
146 the intestines. Fluorescence was relatively weak in flies fed a CD (Fig. 2G), but was far
147 stronger in flies fed a HFD (Fig. 2H). Semi-quantitative analysis revealed that the level of
148 fluorescence was significantly increased in flies fed a HFD (Fig. 2I).
149 Dietary interventions affect the indigenous microbiota. Therefore, we compared germ-free
150 (GF) flies with those that had been reconstituted with a natural microbiota (Fig. 3). The
151 latter flies had been used in all previously described experiments. As mentioned earlier, a

152 HFD induced stem cell proliferation, which could be visualized by labeling ISCs and
153 enteroblasts with GFP using *esg*-Gal4::UAS-GFP. In flies reconstituted with a natural
154 microbiota, there were fewer *esg*$^+$ cells in flies fed a CD (Fig. 3A) than in flies fed a HFD (Fig.
155 3B). By contrast, among GF flies, the number of *esg*$^+$ cells was low in flies fed a CD (Fig. 3C)
156 or HFD (Fig. 3D). Similar results were obtained by quantitative analysis of the number of
157 *esg*$^+$ cells (Fig. 3E). This lack of induction in GF flies was also observed using reporter strains
158 that allowed visualization of *upd3* expression (Fig. 3F–J), indicating that GF flies lack the
159 signal necessary to induce proliferation of ISCs upon HFD feeding. Whereas the upd3 signal
160 was low in flies reconstituted with a native microbiota and fed a CD (Fig. 3F), it was
161 sustainably increased upon HFD feeding (Fig. 3G). By contrast, the upd3 signal was very low
162 in GF flies fed a CD (Fig. 3H) or HFD (Fig. 3I). qRT-PCR revealed that the transcript level of
163 *upd3* was significantly lower in GF flies fed a HFD or CD than in flies reconstituted with a
164 functional microbiota (Fig. 3J).
165 To elucidate the effects of a HFD on the microbiota, we compared the microbiota
166 composition between flies fed a HFD and those fed a CD. A HFD significantly altered the
167 composition of the microbial community in comparison with a CD, as illustrated by the
168 separation in beta diversity by principal coordinate analysis based on unweighted UNIFRAC
169 (Fig. 4A). Linear discriminant analysis effect size (LEfSe) revealed that the orders
170 Enterobacteriales and Caulobacterales were significantly enriched upon HFD feeding. On
171 the other hand, flies fed a CD exhibited enrichment of species belonging to the family
172 Lactobacillaceae, especially from the genus *Pediococcus* (Fig. 4B). To determine whether
173 these alterations in the microbial community were sufficient to induce stem cell activity, we
174 performed a fecal transplantation assay (Fig. 4C–G). Specifically, we transferred the
175 microbiota of flies fed a CD or HFD into GF flies expressing GFP under the control of the esg

176 driver. Transfer of the microbiota from flies fed a CD did not affect the number of esg$^+$ cells
177 after 3 days (Fig. 4C) or 5 days (Fig. 4D). In addition, transfer of the microbiota from flies fed
178 a HFD did not increase the number of these cells after 3 days (Fig. 4E) or 5 days (Fig. 4F).
179 Quantitative analysis of esg$^+$ cells revealed that neither transfer affected stem cell activity in
180 the intestines (Fig. 4G), indicating that alteration of the microbiota composition does not
181 underlie the increase in stem cell activity observed upon HFD feeding.
182 As well as altering the microbiota composition, a HFD changed the bacterial load (Fig. 5).
183 The bacterial load in the intestines was ~2-fold higher in flies fed a HFD than in flies fed a CD
184 (Fig. 5A). Furthermore, a HFD induced mild constipation and consequently the number of
185 fecal spots deposited over 24 h was substantially reduced by ~60–70% (Fig. 5B). In addition,
186 the number of deposited fecal spots was almost 50% lower in GF flies than in flies
187 reconstituted with a functional microbiota. A HFD significantly reduced fecal spot
188 production both in flies reconstituted with a functional microbiota and GF flies. The gut
189 transit time was shortest in flies reconstituted with a functional microbiota and fed a CD,
190 but was increased in flies fed a HFD (Fig. 5C). This effect was more pronounced in GF flies.
191 The intestinal diameter was larger in flies fed a HFD than in flies fed a CD (Fig. 5D-F), which
192 may reflect the increased bacterial mass in the intestines.
193

194 ## Discussion

195 High-fat or lipid-rich diets are thought to be responsible for the development of a plethora
196 of metabolic disorders, including the epidemic increases in obesity and type 2 diabetes. The
197 current study focused on the effects of a HFD on the intestines, which is the first organ
198 exposed to this dietary intervention. We investigated the effects of a HFD on intestinal
199 structure and physiology using *D. melanogaster* as a simple model. We revealed that a HFD

200 induced a substantial increase in stem cell activity in the intestines, leading to altered cell
201 numbers and changes in the cellular composition of this organ. This induction of stem cell
202 activation was completely reliant on a functional intestinal microbiota. A HFD did not
203 increase stem cell activity in GF flies. Moreover, this effect was also dependent on JNK
204 signaling in enterocytes. We assume that JNK signaling transduces this microbiota-
205 dependent signal in enterocytes, leading to production and release of the cytokine upd3.
206 This, in turn, activates JAK/STAT signaling in ISCs and is thus essential for induction of
207 proliferation in these cells. Taken together, activation of JNK signaling in enterocytes upon
208 HFD feeding is completely reliant on the intestinal microbiota. The effects of HFDs on the
209 structural and functional characteristics of the intestines have been reported in several
210 models. Interestingly, different mechanisms appear to underlie the effects of HFDs on stem
211 cell proliferation. In *Drosophila*, diets containing very high cholesterol concentrations
212 significantly increase the abundance of enteroendocrine cells. This is due to a direct
213 interaction with Notch signaling, which leads to preferential production of enteroendocrine
214 cells [7]. Moreover, reduction of the lipid content decreases the proliferation of
215 enteroendocrine tumors. A HFD induces comparable effects in mice, which are mainly
216 characterized by increased cell proliferation in the intestines [33-35]. Beyaz and colleagues
217 [9, 10] reported that a HFD induces stemness of ISCs, which is accompanied by decoupling
218 of stem cell activity from its niche. This effect is opposite to the augmentation of stem cell
219 function observed in response to dietary restriction in the intestines, which is dependent on
220 increased integration into the stem cell niche rather than decoupling [4]. Comparable with
221 the effects of cholesterol in the intestines of *Drosophila*, the effects of a HFD can be traced
222 back to the direct interactions of particular fatty acids with ISCs [10].

223 These previously reported effects of HFDs on stemness are due to direct interactions
224 between specific compounds in these diets (cholesterol or fatty acids) and intestinal cells.
225 This is in contrast with the mechanism by which a HFD promotes stemness in our system,
226 which is indirect because it requires the microbiota. HFDs are associated with a dysbiotic
227 microbiota, which has been causally linked with various pathogenic states. The microbiota
228 is also dysbiotic during aging [27, 28]. Most previous studies focused on the microbiota
229 composition and reported that a shift toward specific bacterial colonizers correlates with
230 the potential for disease development in the host. This appears to be irrelevant in
231 *Drosophila* because fecal transfer experiments failed to recapitulate the enhanced stemness
232 phenotype. Instead, an increased abundance of bacterial colonizers appears to be more
233 relevant. Two factors likely contribute to the increased microbial abundance in response to
234 a HFD: 1) the high-energy content, which facilitates bacterial growth within the intestines,
235 and 2) the increased gut transit time, which reduces fecal output and thus loss of bacteria.
236 The gut transit time was increased and fecal output was reduced in flies fed a HFD, and
237 these changes might underlie the HFD-induced increase in microbial abundance. An
238 increased gut transit time upon HFD feeding is also observed in mice and humans [36-38],
239 indicating that it is a general response to this nutritional intervention and that a HFD is
240 usually associated with an increased bacterial abundance. One consequence of the
241 increased microbial abundance is elevated pressure within the intestinal lumen, leading to
242 mechanical stress on the intestinal structure. This provides another scenario to explain how
243 a HFD increases the stemness of ISCs; specifically, increased pressure induces an increase in
244 stem cell activity in the intestines [39]. The piezo channel in precursors of enteroendocrine
245 cells responds to mechanical stress, and this leads to production of enteroendocrine cells,
246 which is consistent with the results of this study. We also showed that JNK signaling in

247 enterocytes is essential for a suitable cellular response to such stress [40, 41]. This sentinel
248 function of enterocytes is highly relevant because these cells are confronted with a plethora
249 of stress signals and must signal about their state to enable their replacement if necessary
250 [42, 43].
251 In addition to the effects of a HFD on stem cell activity in the intestines, we also found that
252 this dietary intervention induces long-lasting modifications of the intestinal hormonal
253 architecture. A HFD increased the number of enteroendocrine cells for a considerable
254 duration. This observation is consistent with previous reports that a HFD has multiple
255 effects on intestinal function and homeostasis [44] and changes the expression and release
256 of gut hormones [45]. These hormones play a central role in metabolic control and regulate
257 various aspects of intestinal function [46]. We cannot rule out the possibility that feeding of
258 a HFD for even a relatively short duration has long-lasting effects on intestinal homeostasis.
259 In mammals, the substantial and long-lasting effects of short episodes of HFD feeding (e.g.,
260 only 3 days) attenuate major lipid-sensing systems in the gut [47]. HFDs usually reduce
261 appetite via hormonal circuitry [48] to effectively prevent overnutrition [49]. Whereas
262 almost nothing is known about the effects of HFDs on release of gut hormones in
263 *Drosophila*, a plethora of studies have reported such effects in various mammals [50, 51].
264 Chronic exposure to HFDs increases release of the major gut hormone cholecystokinin in
265 rats [52]. Similar effects have been reported for other gut hormones such as glucagon-like
266 peptide 1 [53]; however, the underlying mechanism remains to be elucidated. Few
267 interventions have been shown to change the number of enteroendocrine cells in the
268 intestines [54]. Such a change would not only modify hormonal and metabolic homeostasis,
269 but may also alter the stem cell niche because enteroendocrine cells are highly relevant for
270 maintenance of this important niche [55].

271 Taken together, our results clearly show that a HFD elicits major effects on intestinal
272 structure and function even in the simple model organism *D. melanogaster*. These effects
273 include transient activation of stem cell activity and long-lasting changes to the cellular
274 architecture in the intestines. Moreover, these effects are completely dependent on the
275 microbiota. The stress-sensing JNK signaling pathway appears to be of central importance
276 in the mechanism underlying these effects.

277

278 ## Material and Methods

279

280 **Fly food and husbandry**

281 All flies were raised in vials on sterile standard cornmeal medium containing 5% inactivated
282 yeast (BD Bacto™ yeast extract), 8.6% cornmeal (Mühle Schlingemann, Waltrop,
283 Germany), 5% glucose (Roth, Karlsruhe, Germany), and 1% agar-agar (Roth) in an incubator
284 at 20°C and 65% humidity. At 3–5 days after hatching, adult flies were transferred to fresh
285 sterile standard cornmeal medium or high-fat medium. High-fat medium was exactly the
286 same as standard cornmeal medium except that it contained 20% (w/v) food-grade palm fat
287 (Palmin®). The following fly strains were used in this study: w^{1118} (Bloomington Stock
288 Center), *esg-GFP* (gift from N. Perrimon, Harvard University, USA), amon-Gal4 (gift from C.
289 Wegener, Würzburg, Germany), *UAS-Luc* (gift from M. Markstein, University of
290 Massachusetts, USA), *su(H)GBE-Gal4* (gift from S. Hou, Frederick, USA) *UAS-basket*^{DN}
291 (Bloomington Stock Center 44801), *10XSTAT::GFP* (gift from E. Bach, New York, USA),
292 *20xUAS-IVS-mCD8::GFP* (Bloomington Stock Center 32194), and 4XTRE-DsRed
293 (Bloomington Stock Center 59011).

294

295 **Axenic flies**

296 Flies were allowed to lay eggs on apple juice agar plates containing 2% agar-agar (Roth
297 5210.2) and 50% apple juice (Rewe Bio apple juice) for about 12 h at 25°C to prevent the
298 presence of larvae. Eggs were collected by rinsing the apple juice agar plates with deionized
299 water and transferred to net baskets. Thereafter, the eggs were bleached for 2 min with 6%
300 sodium hypochlorite (Roth, Karlsruhe, Germany) and then washed with 70% ethanol (Roth)
301 and double autoclaved water under sterile conditions. Bleached embryos were placed on
302 sterile standard cornmeal medium. The lack of bacteria in emerged adults was tested by
303 PCR using universal primers targeting bacterial 16S rDNA.

304

305 **Reconstitution of bacteria**

306 A mixture of the following bacterial species, which were cultured as previously described
307 [56], was used to reconstitute the natural microbiota: *Acetobacter pomorum* (OD_{600} = 0.7),
308 *Lactobacillus brevis*^{EW} (OD_{600} = 8), *Lactobacilles plantarum*^{WJL} (OD_{600} = 6), *Enterococcus*
309 *faecalis* (OD_{600} = 0.8), and *Commensalibacter intestini*^{A911T} (OD_{600} = 1.5) (kindly provided by
310 Carlos Ribeiro, Lisbon, Portugal). To prepare the stock solution for recolonization, the
311 following volumes of each liquid culture were combined in a 15 ml falcon tube: 2 ml of *A.*
312 *pomorum*, 0.02 ml of *L. brevis*^{EW}, 0.25 ml of *L. plantarum*^{WJL}, 2 ml of *E. faecalis*, and 1 ml of *C.*
313 *intestini*^{A911T}. The bacterial mixture was centrifuged three times at 3000 rpm for 15 min and
314 repeatedly resuspended in sterile phosphate-buffered saline (PBS). Finally, the mixture was
315 centrifuged at 3000 rpm for 15 min and resuspended in 25% glycerol prepared in sterile PBS.
316 Aliquots of 500 µl were stored at -20°C. A volume of 50 µl of the bacterial mixture was
317 added to the surface of control or high-fat media and allowed to settle for 1 h at room

318 temperature under sterile conditions. Thereafter, 3–5-day-old GF flies were transferred to
319 the corresponding media.
320
321 **Fecal transplantation**
322 Reconstituted *esg*-GFP flies aged 3–5 days were cultured on high-fat or control media for 7
323 days. Subsequently, five flies were homogenized in 300 µl of MRS medium (BD Difco™,
324 Thermo Scientific, Braunschweig, Germany) using a Bead Ruptor 24 (BioLab Products,
325 Bebensee, Germany). Fly debris was removed by centrifugation, the supernatant was mixed
326 with 5% sucrose, and 200 µl of the mixture was applied to sterile filter paper. GF *esg*-GFP
327 flies were allowed to feed on the filter paper for 24 h and then transferred to control media
328 for 5 or 7 days. GFP^+ cells in the anterior midgut region were counted.
329
330 **Body fat quantification**
331 Total body triacylglycerols in flies were measured using a coupled colorimetric assay as
332 described previously [18, 57]. Groups of five females were weighed and homogenized in 1
333 ml of 0.05% Tween-20 using a Bead Ruptor 24 (BioLab Products, Bebensee, Germany).
334 Homogenates were heat-inactivated at 70°C for 5 min, centrifuged, and incubated with
335 triglyceride solution (Thermo Fisher Scientific, Braunschweig, Germany) at 37°C for 30 min.
336 A standard curve was prepared using glyceryl trioleate. Absorbance at 562 nm was
337 measured.
338
339 **Immunohistochemistry**
340 Intestines were dissected in PBS, fixed in 4% paraformaldehyde for 1 h at room
341 temperature, washed three times with PBST (PBS containing 0.1% Triton X-100), and

342 blocked in blocking buffer (PBST containing 5% normal goat serum) for 1 h at room
343 temperature. Thereafter, intestines were incubated with a primary antibody diluted in
344 blocking buffer overnight at 4°C, washed three times, and then incubated with a secondary
345 antibody diluted in PBST overnight at 4°C in darkness. Subsequently, intestines were
346 washed three times with PBST and mounted on slides in Mowiol 40-88. Images were
347 acquired using a fluorescence microscope equipped with Apotome (Carl Zeiss Image Axio
348 Vision, Jena, Germany). The following antibodies were used: anti-prospero from mouse
349 (1:50, Developmental Studies Hybridoma Bank, Iowa City, USA, MR1A), anti-GFP from
350 mouse (1:300, Developmental Studies Hybridoma Bank, Iowa City, USA 8H11), anti-pJNK
351 polyclonal from rabbit (Promega, Mannheim, Germany), Alexa Fluor 488-labeled goat anti-
352 mouse IgG (1:300, Jackson ImmunoResearch, Dianova, Hamburg, Germany), and Alexa
353 Fluor 555-conjugated goat anti-mouse IgG (1:300, Cell Signaling Technology, Frankfurt,
354 Germany).
355
356 **Fluorescence-based quantification of the *in vivo* STAT-GFP reporter**
357 Intestines of 10xSTAT::GFP flies were dissected after CD or HFD feeding for 3 days and
358 immediately fixed in 4% paraformaldehyde and washed three times with 0.1% PBST. All
359 images were stacked with a thickness of 2 µm and an exposure time of 60 ms. Fluorescence
360 of all cells in the field of view was measured using ImageJ. Corrected total cell fluorescence
361 (CTCF) was calculated as follows: CTCF = integrated density – (area of selected cell × mean
362 fluorescence of background readings).
363
364 **Luciferase assay**

365 The luciferase assay was performed as previously described [58] with minor modifications.
366 The intestines of five adult flies per replicate were collected in 150 µl of Glo Lysis Buffer
367 (Promega, Mannheim, Germany, #E2661) and homogenized using a bead mill homogenizer
368 (BioLab Products, Bebensee, Germany) for 2 min at 3.25 m/s. The homogenate was
369 transferred to a new reaction tube and stored at -20°C until further processing. For
370 luciferase measurement, samples were thawed on ice and 50 µl was transferred to a white
371 flat-bottom 96-well plate, with at least one empty well between treatments. Samples were
372 mixed with the same amount of substrate provided by the One Glo Luciferase Assay System
373 (Promega, Mannheim, Germany, #E6110) immediately before signal detection. Luciferase
374 signals were detected using a Tecan plate reader (Tecan, Infinite M200 Pro, Männedorf,
375 Switzerland). A defined control was included on each plate to normalize treatments across
376 plates.
377
378 **Assessment of fecal output**
379 A small piece of CD or HFD supplemented with Brilliant Blue FCF food dye (E133, Ruth,
380 Bochum, Germany) was transferred to the bottom of a vial. A coverslip was placed in the
381 middle of the vial to split it into two halves. Individual flies were trapped in one half,
382 together with the piece of food, and the vial was sealed with a foam plug. Flies were
383 incubated at 20°C for 24 h. Coverslips were scanned. The numbers of fecal spots was
384 counted manually.
385
386 **Assessment of the intestinal transit time**
387 Each well of a 24-well plate was loaded with a small piece of CD or HFD supplemented with
388 Brilliant Blue FCF food dye. Individual flies were starved for 24 h, transferred to the wells,

389 and monitored every 15 min for 3 h. The appearance of the first dyed fecal spot determined
390 the time from food ingestion to egestion in each individual fly, which was referred to as the
391 transit time.
392
393 **RNA extraction and qRT-PCR**
394 Total RNA was extracted from the midgut of adult female flies that had been kept on
395 standard cornmeal medium or high-fat medium. qRT-PCR was performed as described
396 previously [59]. The following primers were used: *upd3* forward (5′-
397 GAGAACACCTGCAATCTGAA-3′) and *upd3* reverse (5′-AGAGTCTTGGTGCTCACTGT-3′).
398 The primers 8FM (5′-AGAGTTTGATCMTGGCTCAG-3′) and Bact515R (5′-
399 TTACCGCGGCKGCTGGCAC-3′) were also used to quantify the bacterial load.
400
401 **16S amplicon sequencing**
402 DNA was isolated from intestines containing fecal material using a DNeasy Blood and
403 Tissue Kit (Qiagen, Hilden, Germany) following the manufacturer's protocol for purification
404 of total DNA from animal tissues and for pretreatment of Gram-positive bacteria. Intestines
405 of 10 individual flies were pooled per sample to generate sufficient material. Extracted DNA
406 was eluted from the spin filter silica membrane with 100 µl of elution buffer and stored at -
407 80°C.

408 16S profiling and MiSeq sequencing were performed as described previously [60, 61] with
409 modifications. The V3-V4 region of the 16S gene was amplified using the dual barcoded
410 primers 341F (GTGCCAGCMGCCGCGGTAA) and 806R (GGACTACHVGGGTWTCTAAT).
411 Each primer contained additional sequences for a 12-base Golay barcode, an Illumina
412 adaptor, and a linker sequence [62]. PCR was performed using Phusion Hot Start Flex 2×

413 Master Mix (NEB, Frankfurt, Germany) in a GeneAmp PCR system 9700 (Applied
414 Biosystems, Thermo Fisher Scientific, Frankfurt, Germany) and the following program: 98°C
415 for 3 min, 30 cycles of 98°C for 20 s, 55°C for 30 s, and 72°C for 45 s, followed by 72°C for 10
416 min and then 4°C hold. PCR was checked by agarose gel electrophoresis. Normalization was
417 performed using a SequalPrep Normalization Plate Kit (Thermo Fisher Scientific,
418 Darmstadt, Germany) following the manufacturer's instructions. Equal volumes of
419 normalized amplicons were pooled and sequenced on an Illumina MiSeq (2 × 300 nt).

420 MiSeq sequence data were analyzed using MacQIIME v1.9.1 [63]. Briefly, all sequencing
421 reads were trimmed to retain only nucleotides with a Phred quality score of at least 20, and
422 then paired-end assembled and mapped onto the different samples using the barcode
423 information. Rarefaction was performed at 34,000 reads per sample to normalize all
424 samples against the minimum shared read count and to account for differential sequencing
425 depth. Sequences were assigned to operational taxonomic units (OTUs) using UCLUST and
426 the Greengenes reference database (gg_13_8 release) with 97% identity. Representative
427 OTUs were picked and assigned to a taxonomy using UCLUST and the Greengenes
428 database. Quality filtering was performed by removing chimeric sequences using
429 ChimeraSlayer and by removing singletons and sequences that failed to align with PyNAST.
430 The reference phylogenetic tree was constructed using FastTree 2. Relative abundance was
431 calculated by dividing the number of reads for an OTU by the total number of sequences in
432 the sample. Unweighted Unifrac beta diversity was calculated and visualized by generating
433 principal coordinate plots. Differentially abundant taxa were assessed using the
434 nonparametric t test. p values were adjusted for multiple testing using the FDR correction.
435 LEfSe [64] was performed using an online tool available at
436 http://huttenhower.sph.harvard.edu/galaxy. LDA denotes taxa based on their contribution

437 to the overall observed differences between groups, i.e., taxa whose abundance was
438 significantly higher in flies fed a HFD than in flies fed a CD.

439

440 **Statistical analysis**

441 All statistical analyses were performed using Prism 6.0 (GraphPad Software, San Diego,
442 USA). Lifespan data were analyzed by the log rank test (Mantel-Cox).

443

444 **Acknowledgments**

445 We thank Britta Laubenstein and Christiane Sandberg for excellent technical help. In
446 addition, we thank Michelle Markstein, Erika Bach, Norbert Perrimon, Stephen Hou, Chris
447 Wegner, and the Bloomington Stock Center for providing flies. This work was supported by
448 the German Research Foundation as part of CRC 1182 (subproject C2) and by the Cluster of
449 Excellence 'Inflammation at Interfaces'.

450

451 **References**

452 1. Ogden CL, Yanovski SZ, Carroll MD, Flegal KM. The epidemiology of obesity.
453 Gastroenterology. 2007;132(6):2087-102. doi: 10.1053/j.gastro.2007.03.052. PubMed PMID:
454 17498505.
455 2. Alonso S, Yilmaz OH. Nutritional Regulation of Intestinal Stem Cells. Annu Rev Nutr.
456 2018;38:273-301. Epub 2018/05/26. doi: 10.1146/annurev-nutr-082117-051644. PubMed
457 PMID: 29799767.
458 3. Haller S, Jasper H. You Are What You Eat: Linking High-Fat Diet to Stem Cell
459 Dysfunction and Tumorigenesis. Cell Stem Cell. 2016;18(5):564-6. doi:
460 10.1016/j.stem.2016.04.010. PubMed PMID: 27152439.
461 4. Yilmaz OH, Katajisto P, Lamming DW, Gultekin Y, Bauer-Rowe KE, Sengupta S, et al.
462 mTORC1 in the Paneth cell niche couples intestinal stem-cell function to calorie intake.
463 Nature. 2012;486(7404):490-5. doi: 10.1038/nature11163. PubMed PMID: 22722868;
464 PubMed Central PMCID: PMCPMC3387287.
465 5. O'Brien LE, Soliman SS, Li X, Bilder D. Altered modes of stem cell division drive
466 adaptive intestinal growth. Cell. 2011;147(3):603-14. doi: 10.1016/j.cell.2011.08.048.
467 PubMed PMID: 22036568; PubMed Central PMCID: PMCPMC3246009.
468 6. Zeituni EM, Wilson MH, Zheng X, Iglesias PA, Sepanski MA, Siddiqi MA, et al.
469 Endoplasmic Reticulum Lipid Flux Influences Enterocyte Nuclear Morphology and Lipid-
470 dependent Transcriptional Responses. J Biol Chem. 2016;291(45):23804-16. doi:

471 10.1074/jbc.M116.749358. PubMed PMID: 27655916; PubMed Central PMCID:
472 PMCPMC5095432.
473 7. Obniski R, Sieber M, Spradling AC. Dietary Lipids Modulate Notch Signaling and
474 Influence Adult Intestinal Development and Metabolism in Drosophila. Dev Cell.
475 2018;47(1):98-111 e5. doi: 10.1016/j.devcel.2018.08.013. PubMed PMID: 30220569.
476 8. Mao J, Hu X, Xiao Y, Yang C, Ding Y, Hou N, et al. Overnutrition stimulates intestinal
477 epithelium proliferation through beta-catenin signaling in obese mice. Diabetes.
478 2013;62(11):3736-46. doi: 10.2337/db13-0035. PubMed PMID: 23884889; PubMed Central
479 PMCID: PMCPMC3806619.
480 9. Beyaz S, Yilmaz OH. Molecular Pathways: Dietary Regulation of Stemness and Tumor
481 Initiation by the PPAR-delta Pathway. Clin Cancer Res. 2016;22(23):5636-41. doi:
482 10.1158/1078-0432.CCR-16-0775. PubMed PMID: 27702819; PubMed Central PMCID:
483 PMCPMC5135602.
484 10. Beyaz S, Mana MD, Roper J, Kedrin D, Saadatpour A, Hong SJ, et al. High-fat diet
485 enhances stemness and tumorigenicity of intestinal progenitors. Nature. 2016;531(7592):53-
486 8. Epub 2016/03/05. doi: 10.1038/nature17173. PubMed PMID: 26935695; PubMed Central
487 PMCID: PMCPMC4846772.
488 11. Nystrom M, Mutanen M. Diet and epigenetics in colon cancer. World J Gastroenterol.
489 2009;15(3):257-63. PubMed PMID: 19140224; PubMed Central PMCID: PMCPMC2653321.
490 12. Reddy BS. Types and amount of dietary fat and colon cancer risk: Prevention by
491 omega-3 fatty acid-rich diets. Environ Health Prev Med. 2002;7(3):95-102. doi:
492 10.1265/ehpm.2002.95. PubMed PMID: 21432290; PubMed Central PMCID:
493 PMCPMC2723490.
494 13. Newmark HL, Yang K, Lipkin M, Kopelovich L, Liu Y, Fan K, et al. A Western-style diet
495 induces benign and malignant neoplasms in the colon of normal C57Bl/6 mice.
496 Carcinogenesis. 2001;22(11):1871-5. PubMed PMID: 11698351.
497 14. Ning Y, Wang L, Giovannucci EL. A quantitative analysis of body mass index and
498 colorectal cancer: findings from 56 observational studies. Obes Rev. 2010;11(1):19-30. doi:
499 10.1111/j.1467-789X.2009.00613.x. PubMed PMID: 19538439.
500 15. Karunanithi S, Levi L, DeVecchio J, Karagkounis G, Reizes O, Lathia JD, et al. RBP4-
501 STRA6 Pathway Drives Cancer Stem Cell Maintenance and Mediates High-Fat Diet-Induced
502 Colon Carcinogenesis. Stem Cell Reports. 2017;9(2):438-50. doi:
503 10.1016/j.stemcr.2017.06.002. PubMed PMID: 28689994; PubMed Central PMCID:
504 PMCPMC5549806.
505 16. Cani PD, Bibiloni R, Knauf C, Waget A, Neyrinck AM, Delzenne NM, et al. Changes in
506 gut microbiota control metabolic endotoxemia-induced inflammation in high-fat diet-
507 induced obesity and diabetes in mice. Diabetes. 2008;57(6):1470-81. doi: 10.2337/db07-
508 1403. PubMed PMID: 18305141.
509 17. Cani PD, Neyrinck AM, Fava F, Knauf C, Burcelin RG, Tuohy KM, et al. Selective
510 increases of bifidobacteria in gut microflora improve high-fat-diet-induced diabetes in mice
511 through a mechanism associated with endotoxaemia. Diabetologia. 2007;50(11):2374-83.
512 doi: 10.1007/s00125-007-0791-0. PubMed PMID: 17823788.
513 18. Hildebrandt MA, Hoffmann C, Sherrill-Mix SA, Keilbaugh SA, Hamady M, Chen YY, et
514 al. High-fat diet determines the composition of the murine gut microbiome independently of
515 obesity. Gastroenterology. 2009;137(5):1716-24 e1-2. doi: 10.1053/j.gastro.2009.08.042.
516 PubMed PMID: 19706296; PubMed Central PMCID: PMCPMC2770164.
517 19. Kim KA, Gu W, Lee IA, Joh EH, Kim DH. High fat diet-induced gut microbiota
518 exacerbates inflammation and obesity in mice via the TLR4 signaling pathway. PLoS One.

519 2012;7(10):e47713. doi: 10.1371/journal.pone.0047713. PubMed PMID: 23091640; PubMed
520 Central PMCID: PMCPMC3473013.
521 20. de La Serre CB, Ellis CL, Lee J, Hartman AL, Rutledge JC, Raybould HE. Propensity to
522 high-fat diet-induced obesity in rats is associated with changes in the gut microbiota and gut
523 inflammation. Am J Physiol Gastrointest Liver Physiol. 2010;299(2):G440-8. doi:
524 10.1152/ajpgi.00098.2010. PubMed PMID: 20508158; PubMed Central PMCID:
525 PMCPMC2928532.
526 21. Daniel H, Gholami AM, Berry D, Desmarchelier C, Hahne H, Loh G, et al. High-fat diet
527 alters gut microbiota physiology in mice. ISME J. 2014;8(2):295-308. doi:
528 10.1038/ismej.2013.155. PubMed PMID: 24030595; PubMed Central PMCID:
529 PMCPMC3906816.
530 22. Fink C, Staubach F, Kuenzel S, Baines JF, Roeder T. Noninvasive analysis of
531 microbiome dynamics in the fruit fly Drosophila melanogaster. Appl Environ Microbiol.
532 2013;79(22):6984-8. Epub 2013/09/10. doi: 10.1128/AEM.01903-13. PubMed PMID:
533 24014528; PubMed Central PMCID: PMCPMC3811555.
534 23. Li X, Watanabe K, Kimura I. Gut Microbiota Dysbiosis Drives and Implies Novel
535 Therapeutic Strategies for Diabetes Mellitus and Related Metabolic Diseases. Front
536 Immunol. 2017;8:1882. doi: 10.3389/fimmu.2017.01882. PubMed PMID: 29326727; PubMed
537 Central PMCID: PMCPMC5742320.
538 24. Tilg H, Moschen AR. Microbiota and diabetes: an evolving relationship. Gut.
539 2014;63(9):1513-21. doi: 10.1136/gutjnl-2014-306928. PubMed PMID: 24833634.
540 25. Backhed F, Ding H, Wang T, Hooper LV, Koh GY, Nagy A, et al. The gut microbiota as
541 an environmental factor that regulates fat storage. Proc Natl Acad Sci U S A.
542 2004;101(44):15718-23. doi: 10.1073/pnas.0407076101. PubMed PMID: 15505215; PubMed
543 Central PMCID: PMCPMC524219.
544 26. Turnbaugh PJ, Ley RE, Mahowald MA, Magrini V, Mardis ER, Gordon JI. An obesity-
545 associated gut microbiome with increased capacity for energy harvest. Nature.
546 2006;444(7122):1027-31. doi: 10.1038/nature05414. PubMed PMID: 17183312.
547 27. Guo L, Karpac J, Tran SL, Jasper H. PGRP-SC2 promotes gut immune homeostasis to
548 limit commensal dysbiosis and extend lifespan. Cell. 2014;156(1-2):109-22. doi:
549 10.1016/j.cell.2013.12.018. PubMed PMID: 24439372; PubMed Central PMCID:
550 PMCPMC3928474.
551 28. Buchon N, Broderick NA, Chakrabarti S, Lemaitre B. Invasive and indigenous
552 microbiota impact intestinal stem cell activity through multiple pathways in Drosophila.
553 Genes Dev. 2009;23(19):2333-44. doi: 10.1101/gad.1827009. PubMed PMID: 19797770;
554 PubMed Central PMCID: PMCPMC2758745.
555 29. Buchon N, Broderick NA, Poidevin M, Pradervand S, Lemaitre B. Drosophila intestinal
556 response to bacterial infection: activation of host defense and stem cell proliferation. Cell
557 Host Microbe. 2009;5(2):200-11. doi: 10.1016/j.chom.2009.01.003. PubMed PMID:
558 19218090.
559 30. Chatterjee N, Bohmann D. A versatile PhiC31 based reporter system for measuring
560 AP-1 and Nrf2 signaling in Drosophila and in tissue culture. PLoS One. 2012;7(4):e34063. doi:
561 10.1371/journal.pone.0034063. PubMed PMID: 22509270; PubMed Central PMCID:
562 PMCPMC3324472.
563 31. Chakrabarti S, Dudzic JP, Li X, Collas EJ, Boquete JP, Lemaitre B. Remote Control of
564 Intestinal Stem Cell Activity by Haemocytes in Drosophila. PLoS Genet. 2016;12(5):e1006089.
565 doi: 10.1371/journal.pgen.1006089. PubMed PMID: 27231872; PubMed Central PMCID:
566 PMCPMC4883764.

567 32. Bach EA, Ekas LA, Ayala-Camargo A, Flaherty MS, Lee H, Perrimon N, et al. GFP
568 reporters detect the activation of the Drosophila JAK/STAT pathway in vivo. Gene Expr
569 Patterns. 2007;7(3):323-31. doi: 10.1016/j.modgep.2006.08.003. PubMed PMID: 17008134.
570 33. Singh A, Balint JA, Edmonds RH, Rodgers JB. Adaptive changes of the rat small
571 intestine in response to a high fat diet. Biochim Biophys Acta. 1972;260(4):708-15. PubMed
572 PMID: 5028118.
573 34. Sagher FA, Dodge JA, Johnston CF, Shaw C, Buchanan KD, Carr KE. Rat small intestinal
574 morphology and tissue regulatory peptides: effects of high dietary fat. Br J Nutr.
575 1991;65(1):21-8. PubMed PMID: 1705145.
576 35. Balint JA, Fried MB, Imai C. Ileal uptake of oleic acid: evidence for adaptive response
577 to high fat feeding. Am J Clin Nutr. 1980;33(11):2276-80. doi: 10.1093/ajcn/33.11.2276.
578 PubMed PMID: 7435405.
579 36. Anitha M, Reichardt F, Tabatabavakili S, Nezami BG, Chassaing B, Mwangi S, et al.
580 Intestinal dysbiosis contributes to the delayed gastrointestinal transit in high-fat diet fed
581 mice. Cell Mol Gastroenterol Hepatol. 2016;2(3):328-39. doi: 10.1016/j.jcmgh.2015.12.008.
582 PubMed PMID: 27446985; PubMed Central PMCID: PMCPMC4945127.
583 37. vd Baan-Slootweg OH, Liem O, Bekkali N, van Aalderen WM, Rijcken TH, Di Lorenzo C,
584 et al. Constipation and colonic transit times in children with morbid obesity. J Pediatr
585 Gastroenterol Nutr. 2011;52(4):442-5. doi: 10.1097/MPG.0b013e3181ef8e3c. PubMed
586 PMID: 21240026.
587 38. Taba Taba Vakili S, Nezami BG, Shetty A, Chetty VK, Srinivasan S. Association of high
588 dietary saturated fat intake and uncontrolled diabetes with constipation: evidence from the
589 National Health and Nutrition Examination Survey. Neurogastroenterol Motil.
590 2015;27(10):1389-97. doi: 10.1111/nmo.12630. PubMed PMID: 26176421; PubMed Central
591 PMCID: PMCPMC4584183.
592 39. He L, Si G, Huang J, Samuel ADT, Perrimon N. Mechanical regulation of stem-cell
593 differentiation by the stretch-activated Piezo channel. Nature. 2018;555(7694):103-6. doi:
594 10.1038/nature25744. PubMed PMID: 29414942; PubMed Central PMCID:
595 PMCPMC6101000.
596 40. Wu H, Wang MC, Bohmann D. JNK protects Drosophila from oxidative stress by
597 trancriptionally activating autophagy. Mech Dev. 2009;126(8-9):624-37. doi:
598 10.1016/j.mod.2009.06.1082. PubMed PMID: 19540338; PubMed Central PMCID:
599 PMCPMC2750887.
600 41. Stronach BE, Perrimon N. Stress signaling in Drosophila. Oncogene.
601 1999;18(45):6172-82. doi: 10.1038/sj.onc.1203125. PubMed PMID: 10557109.
602 42. Zhou F, Rasmussen A, Lee S, Agaisse H. The UPD3 cytokine couples environmental
603 challenge and intestinal stem cell division through modulation of JAK/STAT signaling in the
604 stem cell microenvironment. Dev Biol. 2013;373(2):383-93. doi:
605 10.1016/j.ydbio.2012.10.023. PubMed PMID: 23110761; PubMed Central PMCID:
606 PMCPMC3534909.
607 43. Gervais L, Bardin AJ. Tissue homeostasis and aging: new insight from the fly intestine.
608 Curr Opin Cell Biol. 2017;48:97-105. doi: 10.1016/j.ceb.2017.06.005. PubMed PMID:
609 28719867.
610 44. Little TJ, Horowitz M, Feinle-Bisset C. Modulation by high-fat diets of gastrointestinal
611 function and hormones associated with the regulation of energy intake: implications for the
612 pathophysiology of obesity. Am J Clin Nutr. 2007;86(3):531-41. PubMed PMID: 17823414.
613 45. Richards P, Pais R, Habib AM, Brighton CA, Yeo GS, Reimann F, et al. High fat diet
614 impairs the function of glucagon-like peptide-1 producing L-cells. Peptides. 2016;77:21-7.

615 doi: 10.1016/j.peptides.2015.06.006. PubMed PMID: 26145551; PubMed Central PMCID:
616 PMCPMC4788507.
617 46. Murphy KG, Bloom SR. Gut hormones and the regulation of energy homeostasis.
618 Nature. 2006;444(7121):854-9. doi: 10.1038/nature05484. PubMed PMID: 17167473.
619 47. Cheung GW, Kokorovic A, Lam CK, Chari M, Lam TK. Intestinal cholecystokinin
620 controls glucose production through a neuronal network. Cell Metab. 2009;10(2):99-109.
621 doi: 10.1016/j.cmet.2009.07.005. PubMed PMID: 19656488.
622 48. Gillum MP, Zhang D, Zhang XM, Erion DM, Jamison RA, Choi C, et al. N-
623 acylphosphatidylethanolamine, a gut- derived circulating factor induced by fat ingestion,
624 inhibits food intake. Cell. 2008;135(5):813-24. doi: 10.1016/j.cell.2008.10.043. PubMed
625 PMID: 19041747; PubMed Central PMCID: PMCPMC2643061.
626 49. El-Salhy M, Mazzawi T, Gundersen D, Hatlebakk JG, Hausken T. Changes in the
627 symptom pattern and the densities of large-intestinal endocrine cells following
628 Campylobacter infection in irritable bowel syndrome: a case report. BMC Res Notes.
629 2013;6:391. doi: 10.1186/1756-0500-6-391. PubMed PMID: 24073715; PubMed Central
630 PMCID: PMCPMC3849659.
631 50. Pilichiewicz AN, Little TJ, Brennan IM, Meyer JH, Wishart JM, Otto B, et al. Effects of
632 load, and duration, of duodenal lipid on antropyloroduodenal motility, plasma CCK and PYY,
633 and energy intake in healthy men. Am J Physiol Regul Integr Comp Physiol.
634 2006;290(3):R668-77. doi: 10.1152/ajpregu.00606.2005. PubMed PMID: 16210415.
635 51. Feinle-Bisset C, Patterson M, Ghatei MA, Bloom SR, Horowitz M. Fat digestion is
636 required for suppression of ghrelin and stimulation of peptide YY and pancreatic polypeptide
637 secretion by intraduodenal lipid. Am J Physiol Endocrinol Metab. 2005;289(6):E948-53. doi:
638 10.1152/ajpendo.00220.2005. PubMed PMID: 15998659.
639 52. Spannagel AW, Nakano I, Tawil T, Chey WY, Liddle RA, Green GM. Adaptation to fat
640 markedly increases pancreatic secretory response to intraduodenal fat in rats. Am J Physiol.
641 1996;270(1 Pt 1):G128-35. doi: 10.1152/ajpgi.1996.270.1.G128. PubMed PMID: 8772510.
642 53. van Citters GW, Kabir M, Kim SP, Mittelman SD, Dea MK, Brubaker PL, et al. Elevated
643 glucagon-like peptide-1-(7-36)-amide, but not glucose, associated with hyperinsulinemic
644 compensation for fat feeding. J Clin Endocrinol Metab. 2002;87(11):5191-8. doi:
645 10.1210/jc.2002-020002. PubMed PMID: 12414891.
646 54. Worthington JJ. The intestinal immunoendocrine axis: novel cross-talk between
647 enteroendocrine cells and the immune system during infection and inflammatory disease.
648 Biochem Soc Trans. 2015;43(4):727-33. doi: 10.1042/BST20150090. PubMed PMID:
649 26551720; PubMed Central PMCID: PMCPMC4613519.
650 55. Scopelliti A, Cordero JB, Diao F, Strathdee K, White BH, Sansom OJ, et al. Local control
651 of intestinal stem cell homeostasis by enteroendocrine cells in the adult Drosophila midgut.
652 Curr Biol. 2014;24(11):1199-211. doi: 10.1016/j.cub.2014.04.007. PubMed PMID: 24814146;
653 PubMed Central PMCID: PMCPMC4046228.
654 56. Leitao-Goncalves R, Carvalho-Santos Z, Francisco AP, Fioreze GT, Anjos M, Baltazar C,
655 et al. Commensal bacteria and essential amino acids control food choice behavior and
656 reproduction. PLoS Biol. 2017;15(4):e2000862. doi: 10.1371/journal.pbio.2000862. PubMed
657 PMID: 28441450; PubMed Central PMCID: PMCPMC5404834.
658 57. Hoffmann J, Romey R, Fink C, Yong L, Roeder T. Overexpression of Sir2 in the adult fat
659 body is sufficient to extend lifespan of male and female Drosophila. Aging (Albany NY).
660 2013;5(4):315-27. Epub 2013/06/15. doi: 10.18632/aging.100553. PubMed PMID: 23765091;
661 PubMed Central PMCID: PMCPMC3651523.

662 58. Markstein M, Dettorre S, Cho J, Neumuller RA, Craig-Muller S, Perrimon N. Systematic
663 screen of chemotherapeutics in Drosophila stem cell tumors. Proc Natl Acad Sci U S A.
664 2014;111(12):4530-5. doi: 10.1073/pnas.1401160111. PubMed PMID: 24616500; PubMed
665 Central PMCID: PMCPMC3970492.
666 59. Warmbold C, Uliczka K, Rus F, Suck R, Petersen A, Silverman N, et al.
667 Dermatophagoides pteronyssinus major allergen 1 activates the innate immune response of
668 the fruit fly Drosophila melanogaster. J Immunol. 2013;190(1):366-71. Epub 2012/12/04.
669 doi: 10.4049/jimmunol.1201347. PubMed PMID: 23203927.
670 60. Sommer F, Adam N, Johansson MEV, Xia L, Hansson GC, Bäckhed F. Altered Mucus
671 Glycosylation in Core 1 O-Glycan-Deficient Mice Affects Microbiota Composition and
672 Intestinal Architecture. PLoS One. 2014;9(1):e85254.
673 61. Sommer F, Ståhlman M, Ilkayeva O, Arnemo Jon M, Kindberg J, Josefsson J, et al. The
674 Gut Microbiota Modulates Energy Metabolism in the Hibernating Brown Bear Ursus arctos.
675 Cell Reports. 2016;14(7):1655-61. doi: 10.1016/j.celrep.2016.01.026.
676 62. Caporaso JG, Lauber CL, Walters WA, Berg-Lyons D, Huntley J, Fierer N, et al. Ultra-
677 high-throughput microbial community analysis on the Illumina HiSeq and MiSeq platforms.
678 ISME J. 2012;6(8):1621-4. doi: 10.1038/ismej.2012.8. PubMed PMID: 22402401; PubMed
679 Central PMCID: PMCPMC3400413.
680 63. http://www.wernerlab.org/software/macqiime.
681 64. Segata N, Izard J, Waldron L, Gevers D, Miropolsky L, Garrett WS, et al. Metagenomic
682 biomarker discovery and explanation. Genome biology. 2011;12(6):R60. doi: 10.1186/gb-
683 2011-12-6-r60. PubMed PMID: 21702898; PubMed Central PMCID: PMCPMC3218848.
684

685 ## Figures

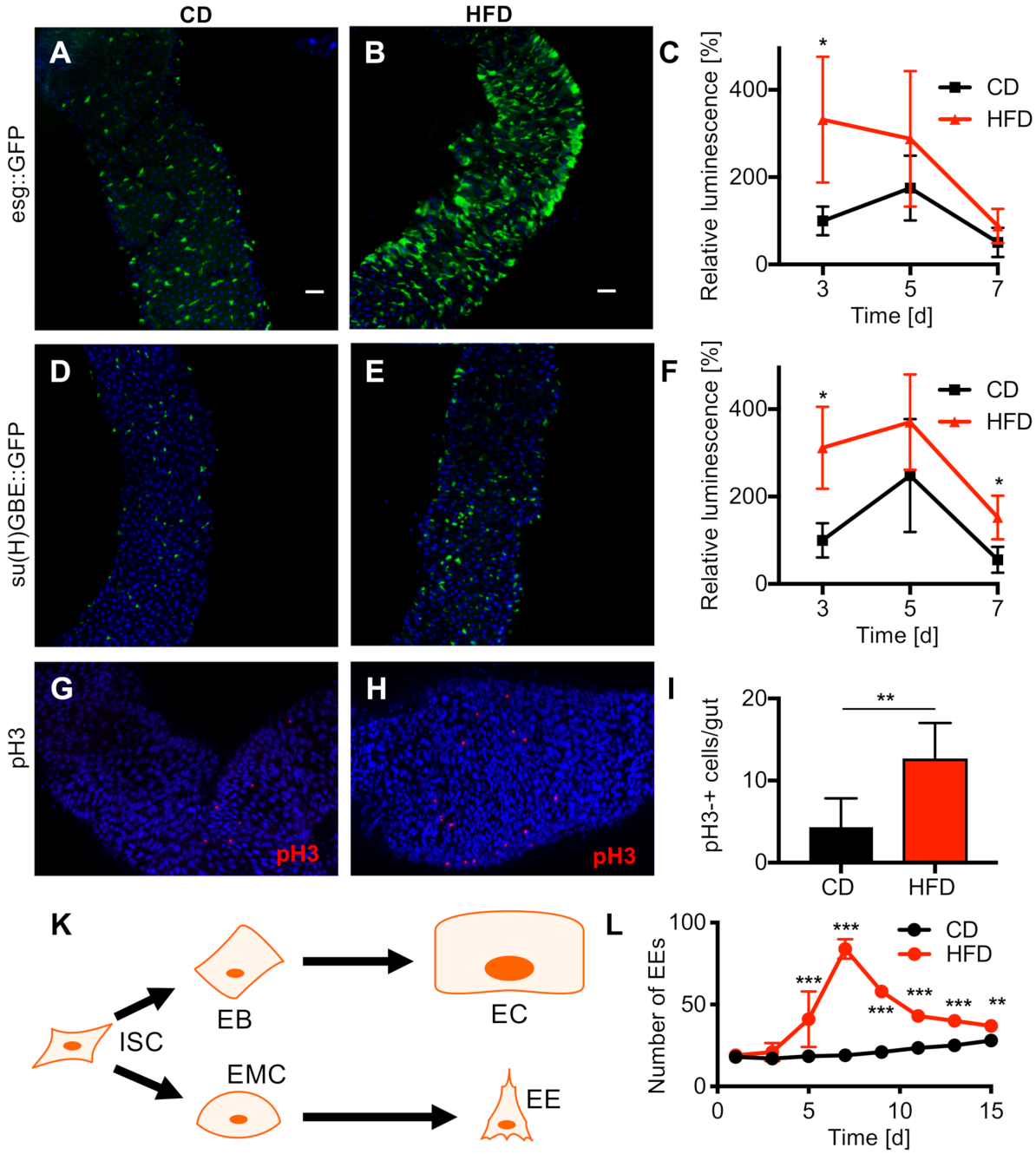

686

687 **Figure 1: A HFD affects the cellular composition in the *Drosophila* intestine.** (A–B)
688 Intestines (anterior midgut R2 region) of flies with labeled ISCs and enteroblasts (*esg-*
689 *Gal4::UAS-GFP*) and fed a CD (A) or a HFD for 3 days (B). (C) Luciferase signals of esg^{+} cells
690 ectopically expressing luciferase (*esg-Gal4::UAS-luciferase*). Intestines were dissected from
691 flies fed a CD or HFD for 3, 5, and 7 days (n = 9–14). (D–E) Pattern of GFP expressed under
692 the control of the enteroblast-specific *su(H)GBE* driver (*su(H)GBE-Gal4::UAS-mCD8-GFP*) in

693 intestines of flies fed a CD (D) or HFD (E). (F) Quantification of luciferase signals in su(H)GBE$^+$
694 cells of flies fed a CD or HFD. (G–H) Representative images of anti-pH3 staining in the R4
695 region of the intestines in female flies fed a CD (G) or HFD (H). (I) Quantification of the
696 number of pH3$^+$ cells in whole intestines (n = 6). (K) Scheme of the generation of various cell
697 types in the *Drosophila* midgut. ISC = intestinal stem cell, EB = enteroblast, EC = enterocyte,
698 EMC = enteroendocrine mother cell, and EE = enteroendocrine cell. (L) Number of
699 enteroendocrine (EE) cells in the R2 region of the intestines over 15 days in flies fed a HFD or
700 CD (n = 10). DAPI was used as a counterstain in all images (scale bar = 50 µm). CD = control
701 diet, HFD = high-fat diet. *p<0.05, **p<0.01, ***p<0.001.
702

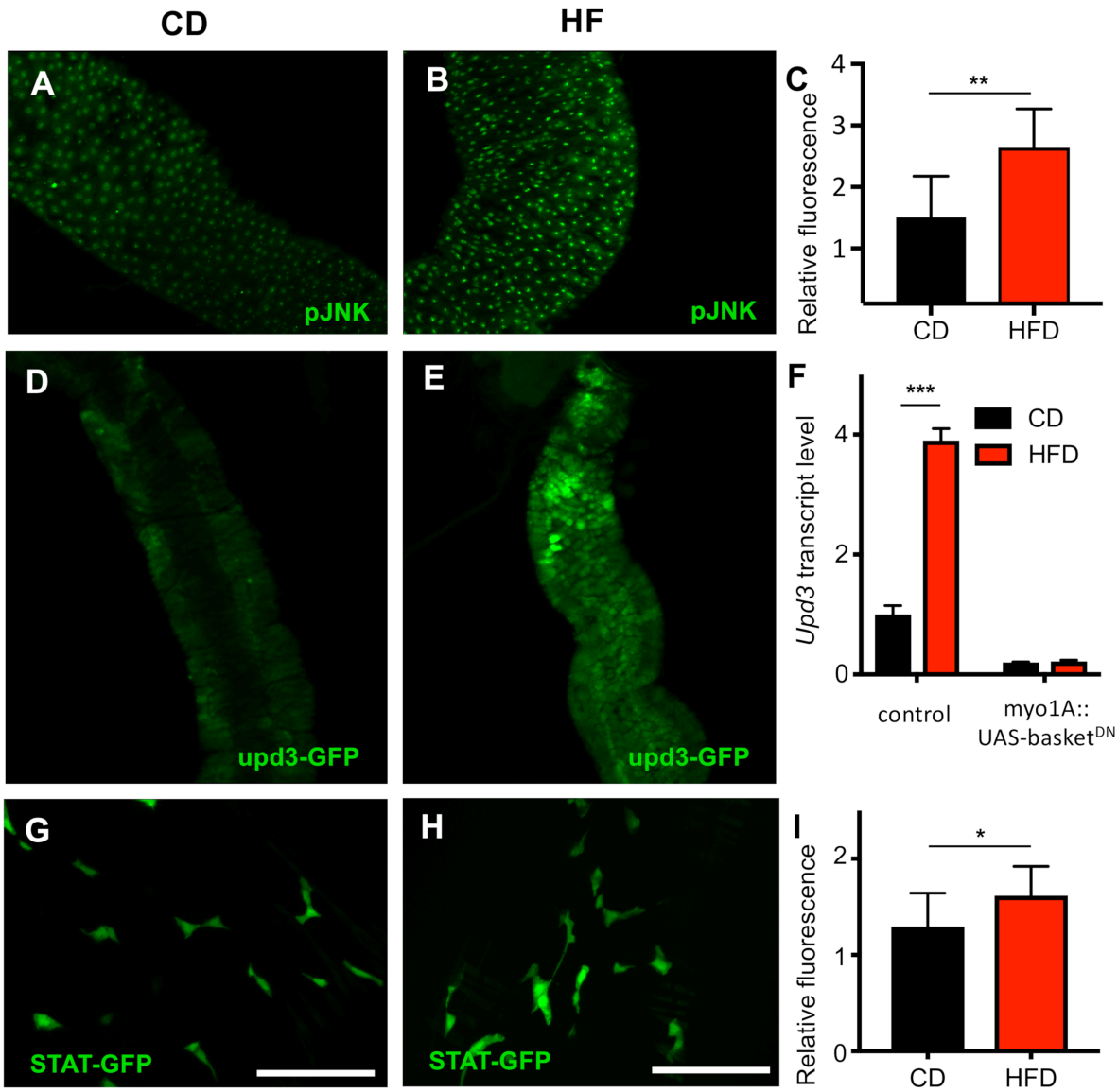

703

704 **Figure 2. A HFD induces *upd3* expression via JNK signaling.** (A–B) Staining with an anti-pJNK
705 antibody in intestines of flies fed a CD (A) or a HFD for 3 days (B). (C) Fluorescence in the
706 anterior midgut of a JNK reporter line (4XTRE-DsRed) fed a CD or HFD (n = 5). (D–E) An *upd3-*
707 *GFP in vivo* reporter was used to monitor upd3 expression in the intestines of flies fed a CD
708 (D) or a HFD for 3 days (E). Representative images of the anterior midgut R2 region of the
709 intestines are shown. (F) qRT-PCR analysis of *upd3* expression in intestines of female flies
710 that expressed a dominant-negative form of basket in enterocytes (*myo1A-Gal4::UAS-*
711 *basket*^{DN}) or the control (*w*^{1118}*::UAS-basket*^{DN}) and fed a CD or a HFD for 3 days (n = 5). (G–H)
712 Images of intestines isolated from a *STAT-GFP in vivo* reporter strain fed a CD (G) or HFD (H)

713 (scale bar = 50µm). (I) Quantification of fluorescence in the *STAT-GFP* reporter strain fed a

714 CD or HFD for 3 days (n = 11). CD = control diet, HFD = high-fat diet. *p<0.05, **p<0.01,

715 ***p<0.001.

716

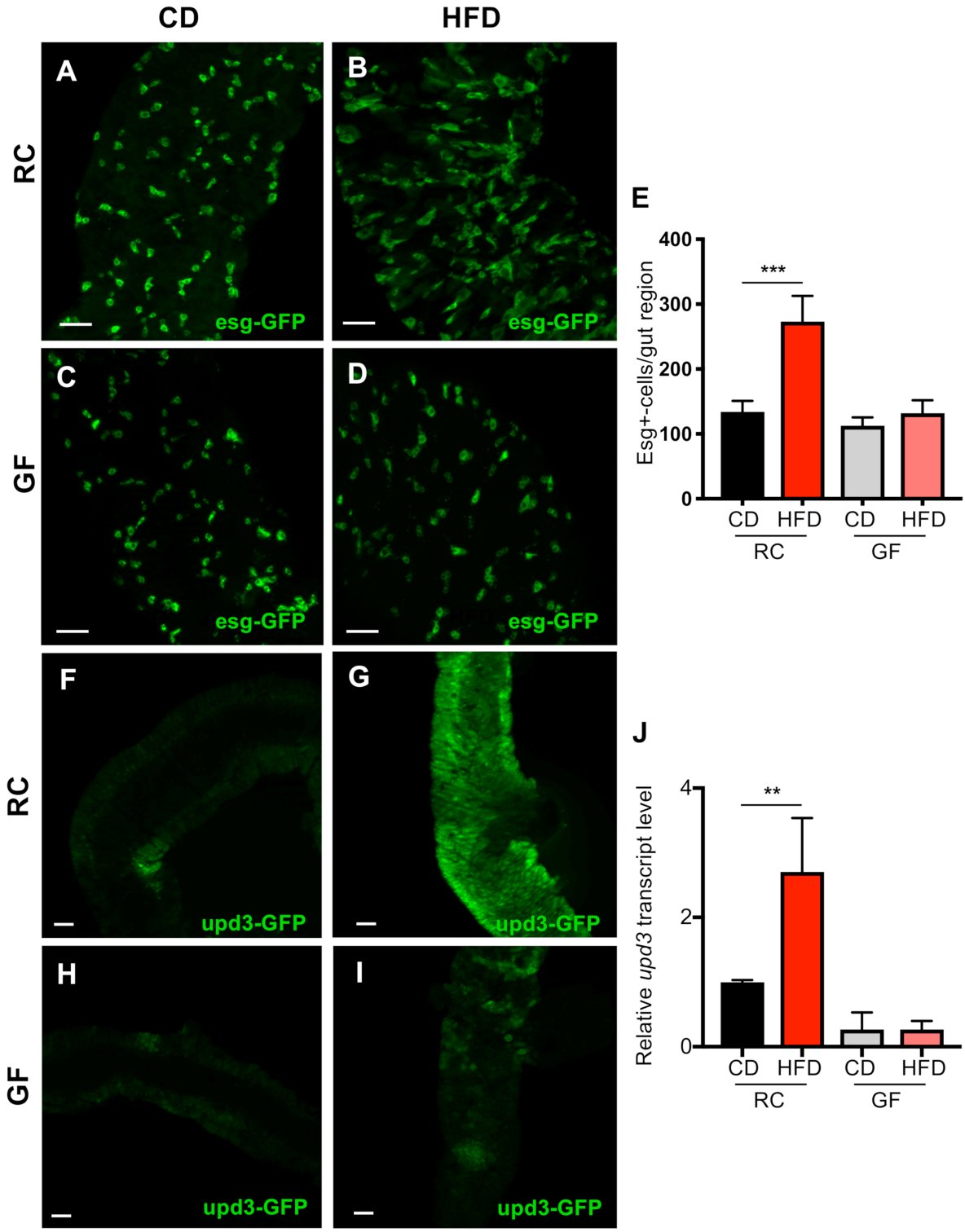

717

718 **Figure 3. HFD-induced cell proliferation and upd3 expression are dependent on the**

719 **intestinal microbiota.** (A–D) The *esg-Gal4::UAS-GFP* strain, in which ISCs and enteroblasts

720 were labeled, was examined. Flies reconstituted with a normal microbiota were fed a CD (A)

721 or HFD (B). GF flies were fed a CD (C) or HFD (D). Representative images of the anterior

722 midgut R2 region are shown (scale bar = 50 µm). (E) Number of *esg*$^{+}$ cells in the R2 region of
723 the intestines (n = 10). (F–I) An *upd3-GFP* reporter was used to examine microbiota-
724 associated modulation of upd3 expression. Flies reconstituted with a normal microbiota
725 were fed a CD (F) or HFD (G). GF flies were fed a CD (H) or HFD (I). Representative images of
726 the R2 region are shown (scale bar = 50 µm). (J) qRT-PCR analysis of *upd3* expression in GF
727 and recolonized flies fed a CD or HFD (n = 5). CD = control diet, HFD = high-fat diet, GF =
728 germ-free, RC = recolonized. **p<0.01, ***p<0.001.
729

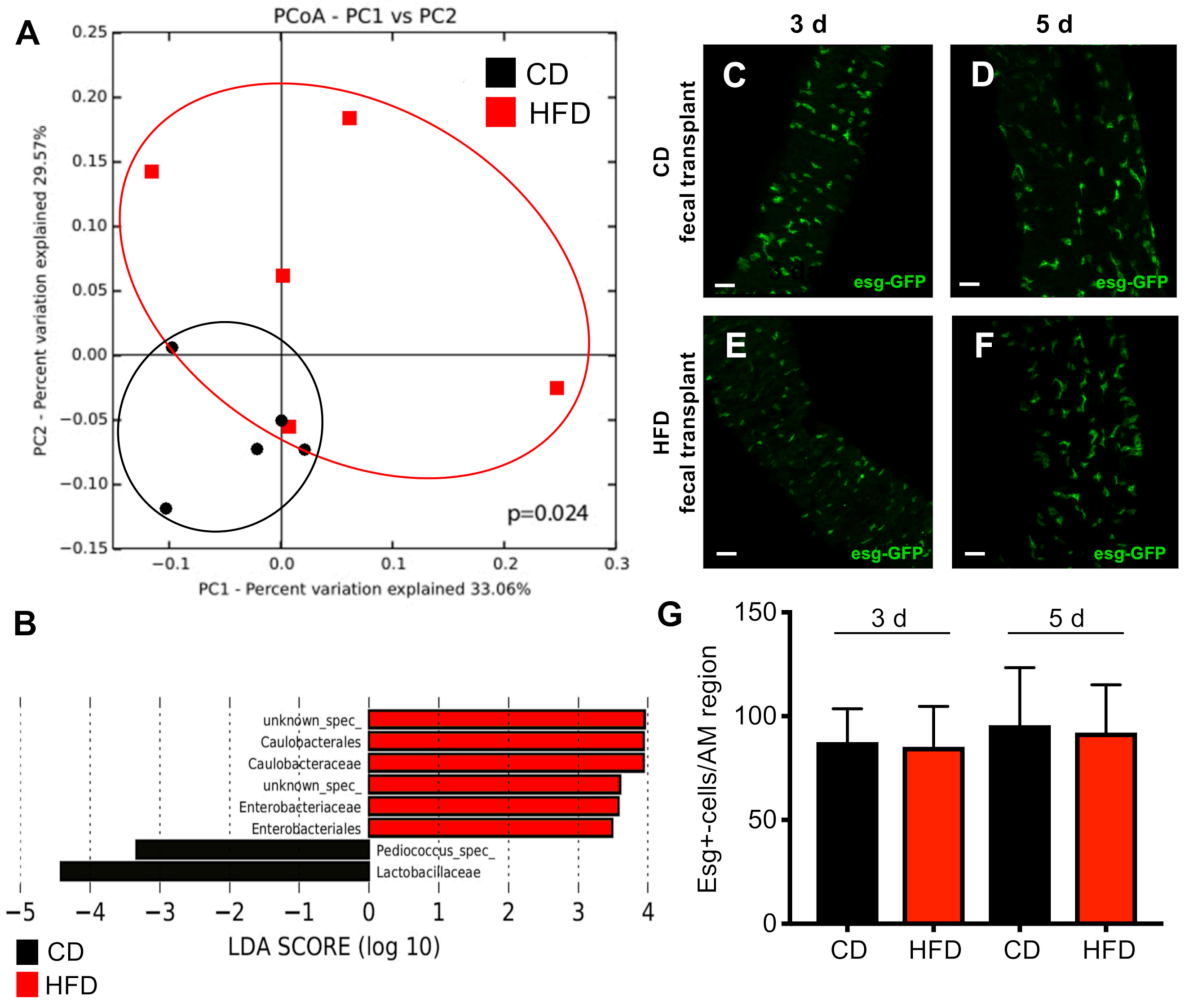

Figure 4. A HFD alters the microbial composition in w^{1118} flies. (A) Principal coordinate analysis showing significant alterations in the intestinal microbiota triggered by a CD or HFD. Each data point corresponds to one biological replicate. (B) Linear discriminant analysis effect size (LEfSe) to determine differentially enriched bacteria in the intestinal microbiota of flies fed a CD or HFD. (C–F) Fecal transplantation into the *esg-Gal4::UAS-GFP* reporter strain was performed to examine the effect of diet-induced changes in the microbial composition on intestinal cell proliferation. Flies were reconstituted with a microbiota derived from flies fed a CD (C–D) or HFD (E–F). Samples were analyzed after 3 days (C and E) or 5 days (D and F) (scale bar = 50 µm). (G) Quantitative analysis of the data presented in (C–F) (n = 8–12). CD = control diet, HFD = high-fat diet.

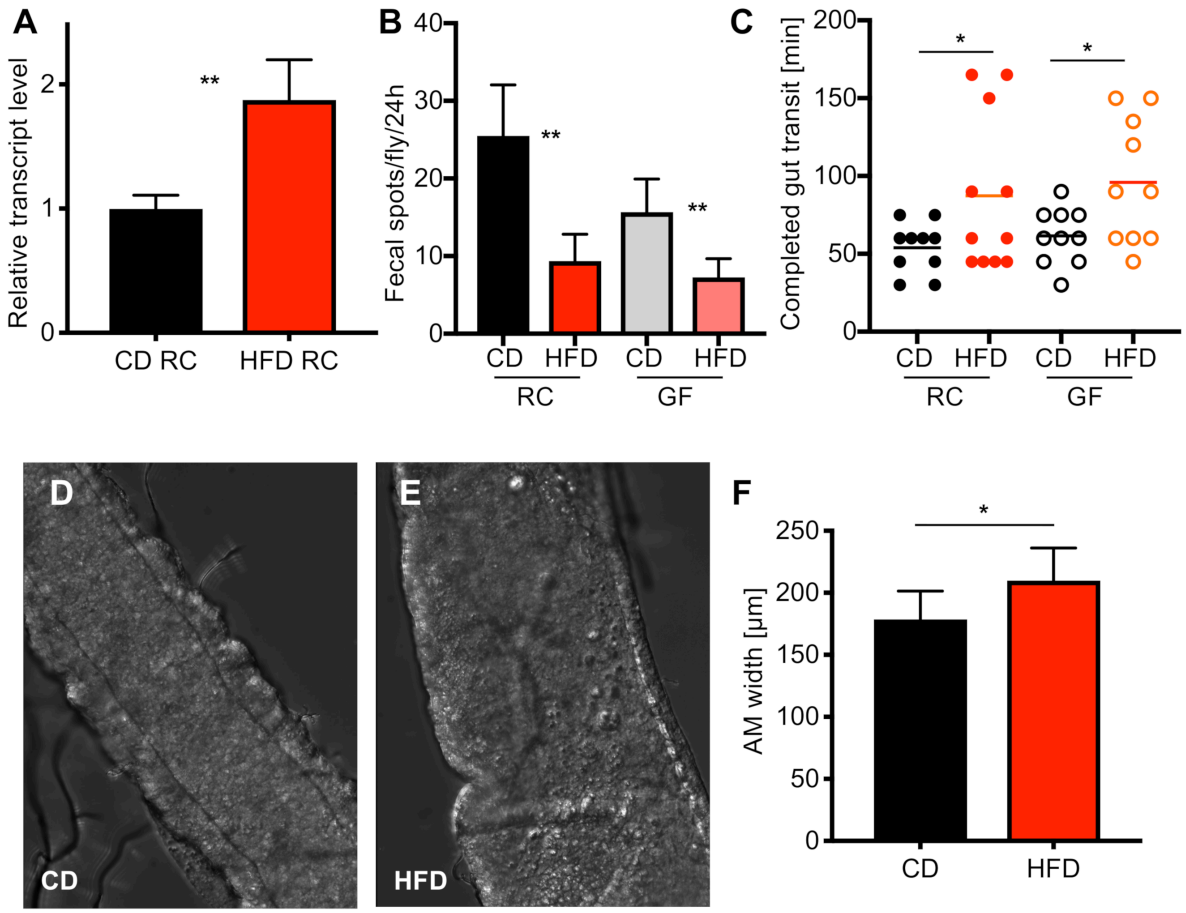

742

743 **Figure 5. A HFD affects egestion and microbial abundance.** (A) The intestinal bacterial load
744 was analyzed by qRT-PCR using 16S universal primers. Intestines were dissected from flies
745 fed a CD or HFD for 3 days (n = 5). (B) Analysis of fecal spot production over 24 h in flies with
746 a reconstituted microbiota and GF flies fed a CD or HFD (n = 7–10). (C) Gut transit time,
747 defined as the time from food ingestion to egestion, was assessed by feeding flies blue food
748 and determining the time until excretion of blue feces (n = 10). (D–E) Representative images
749 of the R2 region of flies fed a CD (D) or a HFD for 3 days (E). (F) Quantification of intestinal
750 thickness (n = 11). CD = control diet, HFD = high-fat diet, GF = germ-free, RC = recolonized.
751 *p<0.05, **p<0.01.